AMERICAN SOCIETY FOR MICROBIOLOGY | Antimicrobial Agents and Chemotherapy®

EXPERIMENTAL THERAPEUTICS

Cyclic Nucleotide-Specific Phosphodiesterases as Potential Drug Targets for Anti-*Leishmania* Therapy

Victor Sebastián-Pérez,[a] Sarah Hendrickx,[b] Jane C. Munday,[c] Titilola Kalejaiye,[c] Ana Martínez,[a] Nuria E. Campillo,[a] Harry de Koning,[c] Guy Caljon,[b] Louis Maes,[b] Carmen Gil[a]

[a]Centro de Investigaciones Biológicas (CIB, CSIC), Madrid, Spain

[b]Laboratory for Microbiology, Parasitology and Hygiene (LMPH), University of Antwerp, Antwerp, Belgium

[c]Institute of Infection, Inflammation and Immunity, College of Medical, Veterinary and Life Sciences, University of Glasgow, Glasgow, United Kingdom

ABSTRACT The available treatments for leishmaniasis are less than optimal due to inadequate efficacy, toxic side effects, and the emergence of resistant strains, clearly endorsing the urgent need for discovery and development of novel drug candidates. Ideally, these should act via an alternative mechanism of action to avoid cross-resistance with the current drugs. As cyclic nucleotide-specific phosphodiesterases (PDEs) of *Leishmania major* have been postulated as putative drug targets, a series of potential inhibitors of *Leishmania* PDEs were explored. Several displayed potent and selective *in vitro* activity against *L. infantum* intracellular amastigotes. One imidazole derivative, compound 35, was shown to reduce the parasite loads *in vivo* and to increase the cellular cyclic AMP (cAMP) level at in a dose-dependent manner at just 2× and 5× the 50% inhibitory concentration (IC_{50}), indicating a correlation between antileishmanial activity and increased cellular cAMP levels. Docking studies and molecular dynamics simulations pointed to imidazole 35 exerting its activity through PDE inhibition. This study establishes for the first time that inhibition of cAMP PDEs can potentially be exploited for new antileishmanial chemotherapy.

KEYWORDS drug discovery, leishmaniasis, cAMP, PDE

The term "leishmaniasis" represents a group of diseases caused by trypanosomatid protozoans that belong to the genus *Leishmania*; more than 20 species in the genus are responsible for these poverty-associated diseases. The clinical outcomes can be grouped into two main forms of the disease: (i) visceral leishmaniasis (VL) caused by *Leishmania donovani* and *L. infantum* and (ii) cutaneous leishmaniasis (CL) caused by *L. major*, *L. tropica*, and *L. mexicana*, among other species. VL is fatal if left untreated, affecting vital organs such as liver, spleen, and bone marrow. In contrast, CL causes the formation of ulcers that may heal spontaneously but leave permanent, disfiguring scars (1, 2). Leishmaniasis is a major health problem in tropical and subtropical countries where the sand fly vector is abundantly present. Although the disease has its main impact in developing countries of Southeast Asia, East Africa, and Latin America, it is also endemic around the Mediterranean Sea (3). The rapid increase in cases of coinfection with HIV, facilitated by the impact of *Leishmania* on the immune system, is an increasing concern (4).

Despite ongoing efforts toward antileishmanial immunotherapy, a promising human vaccine has not yet been developed (5). This fact, together with the challenges in controlling the sandfly vectors (6), ensures that management of this neglected disease continues to rely almost exclusively on chemotherapy. Current treatments include pentavalent antimonials, liposomal amphotericin B, pentamidine, paromomycin, and miltefosine. However, these drugs all have severe drawbacks relating to toxicity, stability, cost, and/or the spread of drug-resistant strains. With the exception of

Received 2 April 2018 **Returned for modification** 30 May 2018 **Accepted** 5 August 2018

Accepted manuscript posted online 13 August 2018

Citation Sebastián-Pérez V, Hendrickx S, Munday JC, Kalejaiye T, Martínez A, Campillo NE, de Koning H, Caljon G, Maes L, Gil C. 2018. Cyclic nucleotide-specific phosphodiesterases as potential drug targets for anti-*Leishmania* therapy. Antimicrob Agents Chemother 62:e00603-18. https://doi.org/10.1128/AAC.00603-18.

Address correspondence to Louis Maes, louis.maes@uantwerpen.be, or Carmen Gil, carmen.gil@csic.es.

TABLE 1 *In vitro* antiparasitic activities of quinazoline-like hPDE7A inhibitors[a]

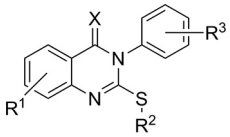

Comp.	X	R^1	R^2	R^3	(IC_{50} [μM]) hPDE7A (25)	MRC-5	*T. cruzi*	*L. infantum*	*T. brucei*	PMM
1	S	H	H	H	0.6	>64.0	51.5	>64.0	60.6	>64.0
2	S	H	Me	2-Br	5.3	3.2	5.0	>64.0	33.4	
3	O	6-Br	H	2,6-diF	11.0	>64.0	>64.0	>64.0	>64.0	
4	O	H	H	H	4.7	>64.0	>64.0	>64.0	37.4	>64.0
5	O	H	Me	2,6-diF	4.7	29.3	>64.0	>64.0	51.7	>64.0
6	O	8-Me	H	2-Br	2.0	>64.0	>64.0	>64.0	>64.0	>64.0
7	O	6-Br	Me	2-Br	0.7	6.7	8.6	26.4	19.4	32.0

[a]IC_{50} data represent inhibition of the growth of *T. cruzi*, *L. infantum*, and *T. brucei* or cytotoxicity toward human lung fibroblasts (MRC-5 cells) and primary peritoneal mouse macrophages (PMM). Each value represents the mean of data from two independent determinations. Comp., compound; hPDE7A, human PDE7A.

miltefosine, all require parenteral administration (7). Alternatives to the current drugs are therefore urgently needed. Ideally, drugs with a novel mechanism of action that are able to overcome resistance to the current drugs and to be delivered by oral administration are desirable (8–10).

Inhibitors of parasite enzymes that are homologous to human enzymes with a well-studied pharmacology may be a good starting point to look for new drugs; as such, target repurposing immediately unlocks a toolbox of potential inhibitors, enzyme structure assays, and assorted other forms of pharmacological and pharmaceutical know-how. With this in mind, human phosphodiesterases (PDEs) are well-studied enzymes essential for cyclic nucleotide signaling, whose druggability has been exploited in various human pathologies, leading to the production of several marketed drugs (11). Specific targeting of parasite PDEs could provide interesting options for the development of PDE inhibitors as antiprotozoal drugs (12, 13). PDEs are responsible for the hydrolysis of cyclic nucleotides, but their signaling role in trypanosomatids is not yet fully understood (14, 15). Since cyclic AMP (cAMP) is clearly involved in the pathogenesis (16), agents able to increase cAMP levels in the parasite, such as PDE inhibitors, may have therapeutic potential (17). Indeed, inhibition of PDEs was shown to lead to runaway cellular cAMP levels and cell death in several protozoan parasites (18–20), but this has yet not been investigated in *Leishmania*.

The *L. major* genome encodes five class I PDEs: *L. major* PDEA (LmjPDEA), LmjPDEB1, LmjPDEB2, LmjPDEC, and LmjPDED (21). LmjPDEA, LmjPDEB1, and LmjPDEB2 were shown to complement a cAMP-PDE-deficient yeast strain, with LmjPDEB1 and LmjPDEB2 being cAMP specific and the activity of LmjPDEA being lower and not fully characterized (22), although its overexpression in *L. donovani* decreased promastigote infectivity with respect to macrophages and impacted resistance to oxidative stress (23). The commercial PDE inhibitors dipyridamole, trequinsin, and etazolate were shown to inhibit LmjPDEB1 and LmjPDEB2 and the proliferation of *L. major* promastigotes *in vitro*; however, due to the high inhibitor concentrations needed for these effects and the omission of a direct demonstration of any perturbation of the cellular cAMP concentration (22), ultimate validation of *Leishmania* PDEs as drug targets is still lacking.

Meanwhile, the X-ray structure of LmjPDEB1 showed a high level of similarity with that of the catalytic site of human PDEs but also revealed a parasite-specific subpocket (p-pocket) near the active site, which could enable the design of parasite-selective inhibitors (24). This area is not accessible to inhibitors in the human PDEs due to a lower volume and changes in the entry residues, which isolate it from the catalytic site. For this reason, this p-pocket would be very useful for the design of selective inhibitors. In *L. major* PDEB1, this domain is formed by residues Met874 to Gly886, which act as its gating residues.

TABLE 2 *In vitro* antiparasitic activities of furan-like hPDE7A inhibitors[a]

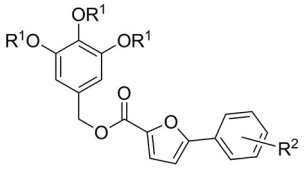

Comp.	R^1	R^2	(IC_{50} [μM]) hPDE7A (26)	MRC-5	*T. cruzi*	*L. infantum*	*T. brucei*	PMM
8	Me	H	5.2	>64.0	>64.0	>64.0	>64.0	>64.0
9	Me	4-Cl,2-NO_2	7.3	35.5	33.0	>64.0	34.0	
10	Me	2,4-diCl	>10[b]	>64.0	>64.0	>64.0	57.4	>64.0
11	Me	4-Me	>10[c]	28.6	>64.0	>64.0	62.9	>64.0
12	Et	H	>10[c]	>64.0	24.5	33.2	30.3	>64.0

[a]IC_{50} data represent inhibition of the growth of *T. cruzi*, *L. infantum*, and *T. brucei* or cytotoxicity toward human lung fibroblasts (MRC-5 cells) and primary peritoneal mouse macrophages (PMM). Each value represents the mean of data from two independent determinations.
[b]38% inhibition at 10 μM.
[c]30% inhibition at 10 μM.

The present report presents selected human PDE inhibitors as pharmacological tools to validate the *Leishmania* PDEs as potential drug targets.

RESULTS

***In vitro* activity.** A small focused library with 30 chemically diverse human cAMP PDE inhibitors, specifically, inhibitors of PDE7A and PDE10A, designed and synthesized in our laboratory was evaluated phenotypically against a panel of three pathogenic trypanosomatids: *Trypanosoma brucei*, *T. cruzi*, and *L. infantum*. Cytotoxicity evaluation was carried out on human lung fibroblasts (MRC-5) and primary peritoneal mouse macrophages (PMM). A first selection included heterocyclic compounds with molecular weights (MW) of <500 Da and different scaffolds, such as quinazolines (Table 1) (25), furans (Table 2) (26), iminothiadiazoles (Table 3) (27), sulfides (Table 4) (28), and imidazoles (Table 5) (29). Only the imidazole compounds showed some inhibitory potential, and to check whether this core could be regarded as a privileged scaffold, 62 imidazole-related compounds from our Medicinal and Biological Chemistry (MBC) library (30) were evaluated next (Table 6). Four hits (compounds 35, 45, 66, and 78) were nontoxic to MRC-5 (50% cytotoxic concentration [CC_{50}], >64 μM), with potent activity against intracellular amastigotes of *L. infantum* and/or *T. cruzi* (Fig. 1). Compounds 66 and 78 showed a 50% inhibitory concentration (IC_{50}) in the same range as that of

TABLE 3 *In vitro* antiparasitic activities of iminothiadiazole-like hPDE7A inhibitors[a]

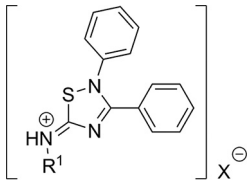

Comp.	R^1	X	(IC_{50} [μM]) hPDE7A (27)	MRC-5	*T. cruzi*	*L. infantum*	*T. brucei*	PMM
13	-CH_2CH_2-OH	Br	1.1	29.3	48.2	32.5	>64.0	32.0
14	-$(CH_2)_2$-Morph	2Br	1.6	30.3	48.3	32.5	60.0	32.0
15	-CH_2-3Pyr	2Br	0.4	7.5	8.1	26.4	35.7	32.0
16	H	Br	1.0	30.1	32.3	32.5	39.2	32.0

[a]IC_{50} data represent inhibition of the growth of *T. cruzi*, *L. infantum*, and *T. brucei* or cytotoxicity toward human lung fibroblasts (MRC-5 cells) and primary peritoneal mouse macrophages (PMM). Each value represents the mean of data from two independent determinations.

TABLE 4 *In vitro* antiparasitic activities of sulfide-like hPDE7A inhibitors[a]

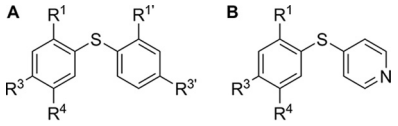

							(IC_{50} [μM])					
Comp.	Form	R^1	R^3	R^4	$R^{1'}$	$R^{3'}$	hPDE7A (28)	MRC-5	*T. cruzi*	*L. infantum*	*T. brucei*	PMM
17	A	NO_2	Cl	H	H	NH_2	0.4	>64.0	>64.0	>64.0	48.0	>64.0
18	B	NO_2	Cl	H			0.7	>64.0	27.2	12.7	19.1	
19	A	NO_2	Cl	H	Br	H	1.0	>64.0	28.8	38.0	32.0	
20	A	NO_2	H	Cl	NHAc	H	2.1	>64.0	50.9	>64.0	>64.0	>64.0
21	A	Cl	NO_2	H	NH_2	H	8.8	35.3	29.0	>64.0	32.6	>64.0
22	A	NO_2	H	Cl	Br	H	1.0	16.9	22.9	51.0	32.9	>64.0
23	B	Cl	NO_2	H			0.2	>64.0	36.7	>64.0	47.3	>64.0

[a]IC_{50} data represent inhibition of the growth of *T. cruzi*, *L. infantum*, and *T. brucei* or cytotoxicity toward human lung fibroblasts (MRC-5 cells) and primary peritoneal mouse macrophages (PMM). Each value represents the mean of data from two independent determinations.

benznidazole (IC_{50} = 3.18 μM) (31) against *T. cruzi*, while compounds 45 and 35 tested against *L. infantum* showed IC_{50}s below that of miltefosine (IC_{50} = 7.56 μM) (31).

***In vitro* metabolic stability.** The selected imidazoles were exposed to mouse S9 microsomal fractions to investigate the *in vitro* metabolic stability through phase I metabolism and phase II metabolism (Table 7). The *T. cruzi* hits corresponding to compounds 66 and 78 were both extensively metabolized through phase I metabolism with, respectively, 5% and 24% of parent drug remaining after 15 min. Phase II metabolism was lower, with 82% and 66% remaining after 15 min and about 50% after 60 min. For the *L. infantum* hits corresponding to compounds 45 and 35, no extensive phase I or phase II metabolism could be demonstrated, indicating satisfactory metabolic stability and suitability for *in vivo* follow-up evaluation. The reference drug diclofenac showed extensive phase I and phase II metabolism, confirming proper functioning of the assay.

Computational studies. To study the binding mode of imidazole compounds 35 and 45 in the LmjPDEB1 catalytic site, docking studies were performed as a starting point for dynamic simulations and were centered on a key residue of the catalytic site, Gln887. For both compounds, the best conformation binds the catalytic site of the enzyme, making key interactions with residues Gln887, Phe857, and Phe890 that allow the formation of a stable protein-ligand complex. In both complexes, the compounds

TABLE 5 *In vitro* antiparasitic activities of imidazole-like hPDE10A inhibitors[a]

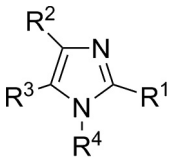

					(IC_{50} [μM])					
Comp.	R^1	R^2	R^3	R^4	hPDE10A (29)	MRC-5	*T. cruzi*	*L. infantum*	*T. brucei*	PMM
24	3,4-diCF_3-Ph	4-OMe-Ph	H	H	0.4	15.4	6.1	32.2	2.0	
25	2-Cl-Ph	4-Br-Ph	4-Br-Ph	H	0.02	>64.0	2.2	50.8	2.2	
26	4-Cl-Ph	4-OMe-Ph	H	H	2.0	19.8	17.8	26.4	29.6	32.0
27	H	4-Br-Ph	4-Br-Ph	H	0.2	42.5	>64.0	32.5	>64.0	32.0
28	2-Br-Ph	4-Br-Ph	4-Br-Ph	H	0.4	>64.0	18.0	>64.0	8.2	>64.0
29	Ph	Ph	Ph	Me	4.1	50.6	8.2	20.6	20.2	>64.0
30	2-Br-Ph	4-OMe-Ph	4-OMe-Ph	H	2.2	>64.0	7.3	14.3	7.5	32.0

[a]IC_{50} data represent inhibition of the growth of *T. cruzi*, *L. infantum*, and *T. brucei* or cytotoxicity toward human lung fibroblasts (MRC-5 cells) and primary peritoneal mouse macrophages (PMM). Each value represents the mean of data from two independent determinations.

TABLE 6 *In vitro* antiparasitic activities of imidazole derivatives from the MBC library[a]

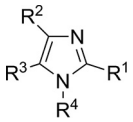

Comp.	R^1	R^2	R^3	R^4	(IC_{50} [μM]) MRC-5	*T. cruzi*	*L. infantum*	*T. brucei*	PMM
31	2-OMe-Ph	4-Br-Ph	4-Br-Ph	H	>64.0	>64.0	48.2	>64.0	48.0
32	3-Cl-Ph	4-Br-Ph	4-Br-Ph	H	45.8	>64.0	7.5	2.0	8.0
33	4-Cl-Ph	4-Br-Ph	4-Br-Ph	H	>64.0	>64.0	20.3	>64.0	20.0
34	Ph	4-Br-Ph	4-Br-Ph	H	>64.0	>64.0	48.2	>64.0	48.0
35	2,4-diOMe-Ph	4-Br-Ph	4-Br-Ph	H	>64.0	7.6	5.2	11.7	>64.0
36	2,5-diOMe-Ph	4-Br-Ph	4-Br-Ph	H	>64.0	17.8	15.0	14.1	>64.0
37	2-OMe-Ph	4-Br-Ph	4-Br-Ph	Bn	>64.0	6.8	6.7	8.1	48.0
38	2-Cl-Ph	4-Br-Ph	4-Br-Ph	Bn	>64.0	14.2	9.4	8.1	36.0
39	2,4-diOMe-Ph	4-Br-Ph	4-Br-Ph	Me	36.4	51.3	18.8	8.2	32.0
40	2,5-diOMe-Ph	4-Br-Ph	4-Br-Ph	Et	>64.0	18.7	16.5	32.5	48.0
41	2-Cl-Ph	4-OMe-Ph	4-OMe-Ph	H	>64.0	7.9	16.5	7.0	32.0
42	2-OMe-Ph	4-OMe-Ph	4-OMe-Ph	H	>64.0	>64.0	48.2	>64.0	48.0
43	Ph	4-OMe-Ph	4-OMe-Ph	H	6.3	8.1	5.9	6.6	48.0
44	2-OMe-Ph	4-OMe-Ph	4-OMe-Ph	Bn	>64.0	4.6	6.7	7.8	36.0
45	2-Cl-Ph	4-OMe-Ph	4-OMe-Ph	Bn	>64.0	5.1	5.1	8.1	48.0
46	Ph	Ph	Ph	H	52.5	>64.0	>64.0	>64.0	>64.0
47	Ph	Ph	Ph	Et	31.2	47.4	42.1	48.3	>64.0
48	Ph	Ph	H	H	55.1	47.9	>64.0	>64.0	>64.0
49	2,4,5-triOMe-Ph	Ph	H	H	19.3	39.2	29.8	25.3	32.0
50	2,4-diOMe-Ph	Ph	H	H	16.6	49.4	35.2	31.0	48.0
51	2,5-diOMe-Ph	Ph	H	H	28.9	33.3	48.2	27.6	48.0
52	2-OMe-Ph	Ph	H	H	30.7	50.6	32.8	58.9	48.0
53	3-Me-Ph	Ph	H	H	30.4	29.5	20.3	27.3	32.0
54	4-F-Ph	Ph	H	H	21.9	48.3	32.5	25.6	32.0
55	4-Me-Ph	Ph	H	H	10.6	28.8	29.9	25.0	32.0
56	2-Cl-Ph	Ph	H	H	37.2	49.1	48.2	>64.0	48.0
57	3-Me-Ph	Ph	H	Bn	>64.0	20.3	26.7	29. 6	>64.0
58	4-Me-Ph	Ph	H	Bn	49.3	7.0	20.4	8.2	32.0
59	2,4,5-triOMe-Ph	Ph	H	Bn	29.0	18.6	12.0	32.5	48.0
60	2-Cl-Ph	Ph	H	Bn	28.5	7.8	53.53	8.345	>64.0
61	Ph	2-naphtyl	H	H	35.7	54.9	36.05	>64.0	36.0
62	Ph	4-OMe-Ph	H	H	13.9	31.8	48.23	37.5	48.0
63	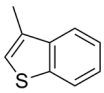	4-OMe-Ph	H	H	4.9	11.5	20.28	25.0	20.0
64	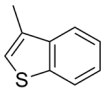	4-Br-Ph	H	H	7.2	7.9	20.28	8.075	20.0
65	Ph	4-Br-Ph	H	H	5.5	8.5	48.2	26.5	48.0
66	2-Pyr	4-Br-Ph	H	H	>64.0	4.7	14.6	14.8	48.0
67	3,5-diCF_3-Ph	4-Br-Ph	H	H	3.5	5.5	2.0	2.00	5.0
68	4-Cl-Ph	4-Cl-Ph	H	H	10.1	8.7	20.3	9.4	32.0
69	4-Cl-Ph	4-Cl-Ph	H	Bn	>64.0	9.1	20.3	9.8	48.0
70	Ph	4-Cl-Ph	H	Bn	61.6	7.7	16.51	8.1	32.0
71	3,5-diCF_3-Ph	3-Pyr	H	H	>64.0	>64.0	48.2	2.0	48.0
72	H	4-OMe-Ph	4-OMe-Ph	H	5.9	46.3	>64.0	>64.0	>64.0
73	H	Me	Ph	H	>64.0	>64.0	>64.0	>64.0	>64.0
74	H	Ph	Ph	H	>64.0	>64.0	>64.0	>64.0	>64.0
75	H	Ph	Ph	Me	>64.0	48.7	35.6	>64.0	48.0
76	H	Ph	Ph	Et	25.8	46.5	32.5	>64.0	32.0
77	H	Ph	Ph	Bu	32.3	22.9	23.7	32.4	48.0
78	H	Ph	Ph	CH_2-4-Cl-Ph	>64.0	4.5	48.0	8.1	>64.0
79	H	Ph	Ph	CH_2-4-CF_3-Ph	>64.0	15.7	42.2	9.0	48.0
80	H	Ph	Ph	CH_2-2-Cl-Ph	14.1	18.2	>64.0	26.9	>64.0

(Continued on next page)

TABLE 6 (Continued)

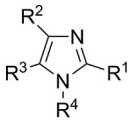

Comp.	R^1	R^2	R^3	R^4	(IC_{50} [μM]) MRC-5	*T. cruzi*	*L. infantum*	*T. brucei*	PMM
81	H	Ph	Ph	Bn	12.2	19.6	38.3	23.2	>64.0
82	H	Ph	Ph	CH_2-biPh	6.7	7.9	36.0	20.7	36.0
83	H	Ph	Ph	CH_2-4-Pyr	44.4	47.4	48.2	32.7	48.0
84	H	Ph	Ph	CH_2-3-Cl-Ph	8.0	20.4	42.2	8.2	48.0
85	H	Ph	Ph	CH_2-4-SMe-Ph	>64.0	>64.0	>64.0	>64.0	>64.0
86	H	Ph	Ph	CO-Ph	>64.0	>64.0	48.2	>64.0	48.0
87	H	Ph	Ph	CH_2-3,4-diCF_3-Ph	6.2	5.0	8.6	8.0	20.0
88	H	4-Br-Ph	H	H	>64.0	47.0	>64.0	>64.0	>64.0
89	H	4-Br-Ph	H	Bn	>64.0	47.8	49.3	32.6	>64.0
90	H	4-Br-Ph	H	CH_2-3,4-diCF_3-Ph	>64.0	>64.0	>64.0	8.7	>64.0
91	H	Ph	H	Bn	48.8	48.7	48.2	58.4	48.0
92	H	4-F-Ph	H	Bn	20.0	48.2	45.6	32.3	48.0

[a]IC_{50} data represent inhibition of the growth of *T. cruzi*, *L. infantum*, and *T. brucei* or cytotoxicity toward human lung fibroblasts (MRC-5 cells) and primary peritoneal mouse macrophages (PMM). Each value represents the mean of data from two independent determinations.

appear to be able to target the parasite-specific pocket, as the docking studies showed the methoxyphenyl substituent of either compound entering the p-pocket (Fig. 2). The best-ranked conformation of compound 35 was selected as the starting point for the molecular dynamics (MD) studies. The results revealed stability of the complex, and to analyze the binding mode in detail, the interactions were monitored during the simulation time of 20 ns. Most of the key interactions found in the docking pose were maintained throughout the run time, confirming that the hydrogen bond with Gln887 and the aromatic interactions with Phe857 and Phe890 provide the stability of the complex. Through this simulation process, it was also possible to identify some interactions with hydrophobic residues from the hydrophobic clamp. Importantly, the methoxy group was able to make a hydrogen bond with a residue inside the p-pocket, Asn881, as early as ns 5 of the simulation, and this interaction was stably maintained during the rest of the simulation process (see Fig. S1 in the supplemental material).

Efficacy in the *L. infantum* BALB/c mouse model. On the basis of the metabolic stability data and their possible interaction with *Leishmania* PDEB1, derivatives 35 and 45 were selected for a proof-of-concept *in vivo* assessment. Both were administered orally in the *L. infantum* BALB/c mouse model at 50 mg/kg of body weight (BW) twice a day (b.i.d.) for 5 days. Amastigote burdens in the liver and spleen target organs were determined on days 16 and 17 of the experiment (Table 8). The results are expressed as Leishman Donovan units (LDU; mean numbers of amastigotes per liver/spleen cell

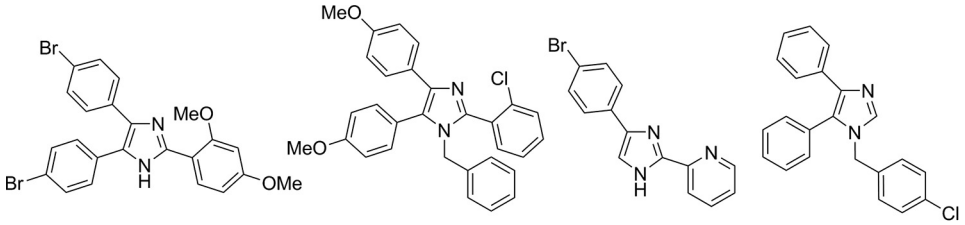

Comp. **35**
IC_{50} (*L.inf*) = 5.2 μM
IC_{50} (*T.cr*) = 7.6 μM
CC_{50} (MRC-5) > 64.0 μM
CC_{50} (PMM) > 64.0 μM

Comp. **45**
IC_{50} (*L.inf*) = 5.1 μM
IC_{50} (*T.cr*) = 5.1 μM
CC_{50} (MRC-5) > 64.0 μM
CC_{50} (PMM) = 48.0 μM

Comp. **66**
IC_{50} (*L.inf*) = 14.6 μM
IC_{50} (*T.cr*) = 4.7 μM
CC_{50} (MRC-5) > 64.0 μM
CC_{50} (PMM) = 48.0 μM

Comp. **78**
IC_{50} (*L.inf*) = 48.0 μM
IC_{50} (*T.cr*) = 4.5 μM
CC_{50} (MRC-5) > 64.0 μM
CC_{50} (PMM) > 64.0 μM

FIG 1 Selected imidazole hits for further studies. Comp, compound.

TABLE 7 *In vitro* metabolic stability: percentage of parent compounds over time in the presence of mouse liver microsomes

Phase I/II	Time (min)	% parent compound remaining upon incubation									
		Comp. 35 (n = 3)		Comp. 45 (n = 3)		Comp. 66 (n = 3)		Comp. 78 (n = 3)		Diclofenac (n = 3)	
		Avg	SD	Avg	SD	Avg	SD	Avg	SD	Avg	SD
CYP_{450}-NADPH (phase I metabolism)	0	100		100		100		100		100	
	15	103	3.6	128	24.6	5	0.8	24	11.5	83	22.7
	30	100	0.5	109	25.8	2	0.2	4	2.8	68	20.5
	60	81	2.0	168	79.5	2	0.2	2	1.5	61	20.4
UGT enzymes (phase II metabolism)	0	100		100		100		100		100	
	15	102	9.4	90	9.2	82	3.0	66	20.8	35	5.9
	30	99	9.4	76	25.6	64	9.3	59	26.9	38	2.1
	60	104	10.8	62	19.3	53	9.9	50	28.7	51	27.8

per milligram of liver/spleen). The vehicle-treated controls showed high amastigote burdens in the liver (LDU = 618 ± 30) and lower burdens in the spleen (LDU = 16 ± 3) since the infection is primarily established in the liver around day 14 postinfection. Oral miltefosine (40 mg/kg once a day [s.i.d.] for 5 days) displayed excellent activity, with parasite burdens in liver and spleen reduced by 98.9% and 96.1%. Upon oral dosing at 50 mg/kg b.i.d. for 5 days, parasite burdens in liver and spleen were reduced by 32.4% and 38.9% for compound 45 and by 36.4% and 57.0% for compound 35.

***In vitro* cAMP measurements in *Leishmania* promastigotes.** To establish whether imidazole 35 induces an increase in intracellular cAMP levels in *L. infantum* promastigotes, the cAMP response was tested at concentrations corresponding to 2× and 5× its IC_{50} against intracellular amastigotes. The experiment was performed on promastigotes since it is not possible to measure cAMP levels for intracellular amastigotes, with their cAMP content masked by that of the host cells, or to obtain sufficient numbers of amastigotes from the infected animals without some host cell contamination. The chosen concentrations had no effect on promastigote viability over the 3 h of the experiment. The compound induced a significant and dose-dependent increase in cellular cAMP levels in the promastigotes (Fig. 3), consistent with inhibition of one or more PDEs in the same concentration range as its antileishmanial effects. The tetrahydrophthalazinone NPD0001, a potent inhibitor of *T. brucei* PDEB1 (TbrPDEB1) and TbrPDEB2 (18, 32), was used as a positive control for a strong cAMP response.

DISCUSSION

One major health problem in tropical and subtropical countries is leishmaniasis, which is also endemic in the Mediterranean area. Although effective drugs exist for

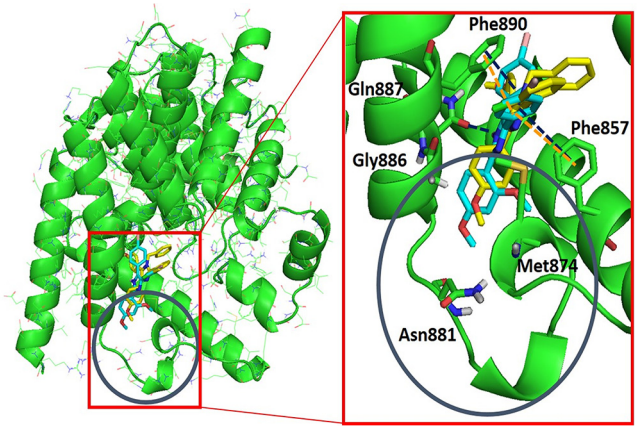

FIG 2 Docking results for imidazole compounds 35 (cyan) and 45 (yellow) in LmjPDEB1. A global view of the protein and a zoomed view of the catalytic binding site, key residues, and the p-pocket (in a gray circle) are shown.

TABLE 8 *In vivo* activity of imidazoles 45 and 35 in the *L. infantum* BALB/c mouse model with respect to organ burden and percentage of efficacy

	Amastigote burden			
	Liver		Spleen	
Dosing group	Mean ± SD LDU	% reduction	Mean ± SD LDU	% reduction
G1 (vehicle [PEG 400])	618 ± 30		16 ± 3	
G2 (miltefosine at 40 mg/kg s.i.d. p.o.[a] for 5 days)	7 ± 2	98.9	1 ± 0	96.1
G3 (Comp. 45 at 50 mg/kg b.i.d. p.o. for 5 days)	418 ± 56	32.4	10 ± 2	38.9
G4 (Comp. 35 at 50 mg/kg b.i.d. p.o. for 5 days)	393 ± 28	36.4	7 ± 1	57.0

[a]p.o., orally.

therapy, the side effects and the spread of drug-resistant strains make the discovery of novel drugs with a new mechanism of action urgent. It is increasingly argued that the search of new leishmanicidal agents should be based on well-known targets with established pharmacology, as such target repurposing greatly speeds up the drug discovery process; the cAMP PDEs fall into that category. The similarity between the human and protozoan enzymes, together with the availability of human PDE inhibitors as reputable therapeutics, paved the way for the development of specific inhibitors of protozoan PDEs as potential drugs (33).

On the basis of this reasoning and of the powerful results obtained by the repurposing of human drugs for antitrypanosomatid therapy (34), 30 known inhibitors of human PDEs from our in-house library were initially selected and tested in a primary *in vitro* screening against a broad panel of pathogens and mammalian cell lines (Tables 1 to 5). Within our experience in the design and development of specific cAMP-hPDE inhibitors, this study specifically aimed at the identification of novel scaffolds for inhibition of protozoan PDEs. The finding that imidazoles with multiple phenyl substitutions showed a tendency to inhibit trypanosomatid growth triggered a subsequent screen of a larger focused library composed of 62 structurally related imidazoles (Table 6) and produced four hits (compounds 35, 45, 66, and 78). These compounds showed promising *in vitro* activity against *L.*

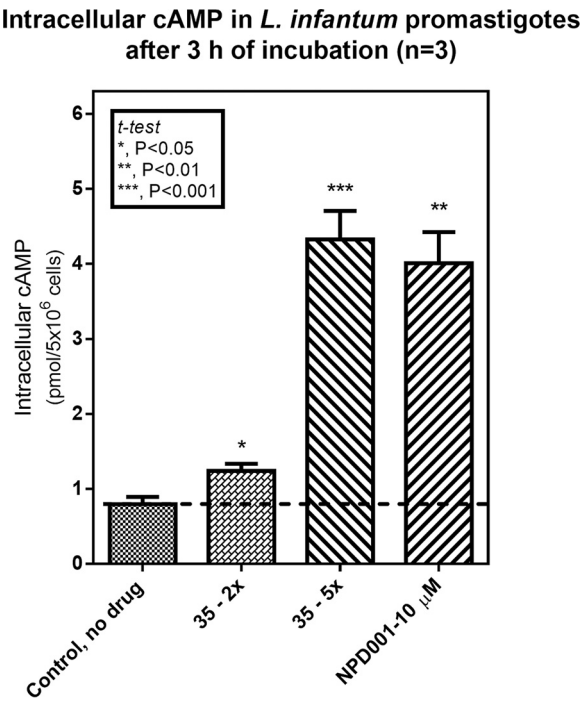

FIG 3 Intracellular cAMP in *L. infantum* promastigotes after 3 h of incubation. Imidazole 35 was used at 2× and at 5× the IC_{50} concentration of 5.1 μM.

infantum or *T. cruzi* intracellular amastigotes, with adequate selectivity with respect to cytotoxicity in MRC-5 cells (selectivity index [SI], >12) (Fig. 1).

The metabolic stability of compounds in early drug development is one of the drug-like properties used in candidate prioritization for progression (35) and directly supports *in vivo* follow-up experiments. To evaluate their suitability for *in vivo* evaluation, the *in vitro* metabolic stability of the hit compounds was assessed using mouse S9 microsomal fraction, with the results showing acceptable stability for both compound 35 and compound 45 (Table 7).

To investigate whether the selected compounds are able to bind the PDE catalytic site, molecular modeling approaches were employed using the published LmjPDEB1 crystal structure (2R8Q) (24). Note that the *L. major* and *L. infantum* PDEB1s are almost identical, displaying identity levels of 95.7% between the full-length open reading frames and 97.4% for the catalytic domains (see Fig. S2 in the supplemental material).

Docking calculations followed by molecular dynamics simulations evidenced that these imidazole compounds are able to bind the active site of *Leishmania major* PDEB1. In addition to interactions with the expected conserved residues, such as the hydrogen bond with Gln887 and the aromatic interactions with Phe857 and Phe890, both compounds were able to target the parasite-specific pocket through a bond between their methoxyphenyl substituent and residue Asn881. This interaction with the p-pocket is crucial for specificity with respect to human PDEs and was maintained during a molecular dynamics simulation (Fig. 2), opening new avenues for the specific design of PDE parasitic inhibitors. To confirm that the effect of the compounds was indeed the result of PDE inhibition in the parasite, a measurable increase in cellular cAMP levels should occur. Consistent with this expectation, imidazole 35 induced a significant dose-dependent increase in the intracellular cAMP content of *L. infantum* promastigotes at concentrations just above the antileishmanial IC_{50}, reaching a level similar to that seen with the potent reference inhibitor NPD0001 (Fig. 3).

Metabolically stable imidazoles were advanced to the *L. infantum*-infected mouse model. Oral treatment of 50 mg/kg of body weight b.i.d. for 5 days with compound 35 or 45 resulted in a 30% to 60% reduction in the parasite burden, which represents only moderate *in vivo* activity compared to that of miltefosine (Table 8). Yet these results encourage further efforts toward optimization of the hit compounds by structure-aided medicinal chemistry, in order to improve drug-like properties such as oral bioavailability.

In conclusion, this is the first time that a PDE inhibitor with a confirmed correlation between *in vitro* antileishmanial activity and cAMP content was shown to exhibit *in vivo* activity, which constitutes an important step toward establishing *Leishmania* PDEs as drug targets. On the basis of these results, imidazole derivatives can be regarded as promising hits to be developed in a hit-to-lead program to obtain new drug candidates for leishmaniasis with a better and safer pharmaceutical profile.

MATERIALS AND METHODS

Ethics statement. The use of laboratory rodents was carried out in strict accordance to all mandatory guidelines (EU directives, including the Revised Directive 2010/63/EU on the Protection of Animals used for Scientific Purposes that came into force on 1 January 2013 and the declaration of Helsinki in its latest version) and was approved by the ethical committee of the University of Antwerp, Belgium [UA-ECD 2016-54 (02/09/2016)].

Compounds studied. All the compounds tested in this work had a purity level of ≥95% by high-performance liquid chromatography (HPLC) and are collected in the MBC library (30). The following compounds were prepared in the Centro de Investigaciones Biológicas (CIB-CSIC) using procedures described previously in the indicated references: quinazolines (compounds 1 to 7) (25), furans (compounds 8 to 12) (26), iminothiadiazoles (compounds 13 to 16) (36), sulfides (compounds 17 to 23) (28), and imidazoles (compounds 24 to 92) (29).

***In vitro* parasite growth inhibition assays.** Integrated screening was used to define the activity profiles of the test compounds (compounds 1 to 92), adopting standard assay protocols as previously described (37). A brief description of each model is given. (i) *Leishmania* amastigotes harvested from the spleen of infected donor hamsters were used for infection. Murine peritoneal macrophages were obtained after intraperitoneal stimulation with 2% starch–water for 24 to 48 h and plated in 96-well

microplates at 10^4 cells/well. After 10^5 amastigotes were added per well and after 5 days of incubation, parasite burdens were microscopically assessed after Giemsa staining. (ii) African trypanosome bloodstream forms of a drug-sensitive *T. brucei* strain were axenically grown in Hirumi-9 medium at 37°C under an atmosphere of 5% CO_2. Assays are performed in 96-well tissue culture plates, with each well containing 10^4 parasites. After 4 days of incubation, parasite growth was assessed by adding resazurin and fluorimetric reading after 4 h at 37°C. (iii) For a Chagas disease-related model, a nifurtimox-sensitive Tulahuen strain (LacZ transfected) of *T. cruzi* was maintained on MRC-5 cells. Assays were performed in 96-well tissue culture plates, with each well containing the compound dilutions together with 3×10^3 MRC-5 cells and 3×10^4 trypomastigotes. After 7 days of incubation, colorimetric reading was performed after addition of chlorophenol red beta-D-galactopyranoside as the substrate. (iv) For a cytotoxicity model, MRC-5 cells were cultured in minimal essential medium (MEM) supplemented with 20 mM L-glutamine, 16.5 mM $NaHCO_3$, and 5% fetal calf serum. Assays are performed at 37°C and 5% CO_2 in 96-well tissue culture plates with confluent monolayers. After 7 days of incubation, cell proliferation and viability were assessed after addition of resazurin and fluorescence reading.

Microsomal stability assays. Mouse liver microsomes (S9), NADPH-generating system solutions, and uridine glucuronosyl transferase (UGT) reaction mix (BD Biosciences) were kept at −80°C. The test compounds (compounds 35, 45, 66, and 78), the internal standard tolbutamide, and the reference compound diclofenac were formulated in dimethyl sulfoxide (DMSO) at 10 mM. The assay was carried out based on the BD Biosciences guidelines for use (TF000017 Rev1.0) with minor adaptations. The metabolic stability of the compounds was studied through the use of members of the CYP_{450} superfamily (phase I metabolism) by fortification with NADPH and through the use of uridine glucuronosyl transferase (UGT) enzymes (phase II metabolism) by fortification with UDP glucuronic acid (UDPGA). For CYP_{450} and other NADPH-dependent enzymes, the compounds were incubated at 5 μM together with 0.5 mg/ml S9–potassium phosphate buffer in a reaction started by the addition of 1 mM NADP. At defined time points, 20 μl was withdrawn from the reaction mixture and 80 μl cold acetonitrile (ACN) was added to inactivate the enzymes and precipitate the protein. The mixture was subjected to vortex mixing for 30 s and centrifuged at 4°C for 5 min to collect the supernatant. For UGT enzymes, the compounds were incubated at 5 μM together with 0.5 mg/ml S9 in a reaction started by the addition of 2 mM UDPGA cofactor. The loss of the parent compound was determined using ultraperformance liquid chromatography (UPLC) and a Waters Acquity system coupled with tandem quadrupole mass spectrometry (MS^2) (Waters Xevo), equipped with an electrospray ionization (ESI) interface, and operated in multiple-reaction-monitoring (MRM) mode.

Docking studies. Compounds 35 and 45 were prepared and converted into three-dimensional (3D) data for computational studies using the Ligprep tool (38), a module of the Schrödinger software package. All possible states at the target pH of 7.0 ± 1 were generated, and stereoisomers and low-energy ring conformations were allowed during the process. The crystal structure (24) of LmjPDEB1 was retrieved from the Protein Data Bank (PDB 2R8Q) and prepared using the Protein Preparation Wizard tool (39) implemented on Maestro (40). Automated docking was used to assess the appropriate binding orientations and conformations of the ligand. A Lamarckian genetic algorithm (41) method implemented in the program AutoDock 4.2 (42) was employed. For docking calculations, Gasteiger charges were added, rotatable bonds were set by the use of AutoDock tools (ADT), and all torsions were allowed to rotate for the ligand. In all cases, we used grid maps with a grid box size of 60-by-60-by-60 $Å^3$ points and a grid-point spacing of 0.375 Å, using Gln887 as the centroid of the grid. The docking protocol consisted of 100 independent Genetic Algorithm (GA) runs, a population size of 150, and a maximum of 250,000 evaluations, while the other parameters were defaults. The final best-docked clusters, within the default 2.0-Å root mean square deviation (RMSD), according to the binding energies and relative population data provided by Autodock, were analyzed by visual inspection. In both complexes, two main clusters were found in terms of energy and were also the most highly populated ones, and those clusters were therefore selected for further analysis (Fig. S3 and S4).

Molecular dynamics (MD) studies. An Optimized Potentials for Liquid Simulations-2005 (OPLS2005) (43) force field was used as the force field in a Desmond molecular dynamics system (44) to study the behavior of the ligand-target complex. The protein-ligand complexes obtained from the AutoDock docking protocol were prepared using the Desmond setup wizard. For ligand 35, QMESP charges were calculated using Jaguar software (45), carrying out a geometry optimization with the basis set CC-PVTZ++. Charges were added to the best docking output pose for further use. The system was solvated in a triclinical periodic box of simple point-charge (SPC) water and then neutralized using an appropriate number of counter ions. Also, a physiological NaCl concentration of 0.15 M was added in the system builder. The method selected for MD was NPT (Noose-Hover chain thermostat [at 300 K; Martyna-Tobias-Klein barostat at 10.1325^5 pascals]); no constraints were applied in the MD protocol. Energy minimization of the prepared system was done using up to a maximum of 10 steps and the steepest-descent method or until a gradient threshold (25 kcal/mol/Å) was reached. The default Desmond protocol was used to equilibrate the system. Further MD simulations were carried out on these equilibrated systems for a time period of 20 ns. The quality of MD simulations was assessed using the Simulation Quality Analysis tools and analyzed by the Simulation Event Analysis tool, and ligand-receptor interactions were identified using the Simulation Interaction Diagram tool. Energy fluctuations, RMSD, and root-mean-square fluctuations (RMSF) of the complexes in each trajectory were analyzed with respect to simulation time. Visualization and analysis of the dynamics trajectories were performed using both Visual Molecular Dynamics (VMD) (46) and Desmond Maestro simulation analysis tools.

cAMP determination in *Leishmania* promastigotes. Incubations of promastigotes were performed in 24-well plates with either 2× or 5× the IC_{50} of compound 35 for 3 h and were initiated by adding 15

μl of each compound, at a concentration of 100× in 100% DMSO, to reach a level of 1.5 ml of culture. A 1.5-ml control culture received 15 μl of solvent (100% DMSO). After 3 h, a sample containing 5×10^6 cells was taken from each well and centrifuged at 4,500 × *g* for 10 min at 4°C and the supernatant was carefully removed. For quantification of the intracellular cAMP, the cell pellet was immediately resuspended in 100 μl 0.1 M HCl (by repeated up-and-down pipetting) and incubated on ice for 20 min in order to obtain complete cell lysis. The suspensions were then centrifuged at 10,300 × *g* in a microcentrifuge for 10 min at 4°C, and the supernatant (lysate) was transferred to a fresh microcentrifuge tube that was stored at −20°C. The experiment was performed three times independently, and all samples were assayed in duplicate using a direct cyclic AMP enzyme immunoassay kit (Assay Designs) according to the manufacturer's instructions.

Efficacy potential in the *L. infantum* BALB/c mouse model. Female BALB/c mice (body weight [BW], approximately 20 g) were purchased from a commercial source (Janvier Labs, France) and kept in quarantine for at least 5 days before the experiment was started. Food and drinking water were available for laboratory rodents *ad libitum*. The mice were randomly allocated to experimental units of 6 animals/group based on live BW at the start of the experiment (day 0 = day of infection). Spleen-derived *L. infantum* amastigoteswere purified using two centrifugation steps and diluted for preparation of an infection inoculum containing 2×10^7 amastigotes/100 μl phosphate-buffered saline (PBS). The infection inoculum was administered by slow intravenous injection in the tail vein. The test compounds (compounds 35 and 45) were formulated in polyethylene glycol (PEG 400) at 25 mg/ml for a planned dosing level of 50 μl/25 g. Miltefosine was formulated in water at 10 mg/ml for a planned dosing level of 100 μl/25 g. The 5-day oral treatment started at day 7 postinfection and involved 4 groups: group 1 (G1; PEG 400 vehicle b.i.d.), G2 (miltefosine at 40 mg/kg of body weight s.i.d.), G3 (compound 45 at 50 mg/kg b.i.d.), and G4 (compound 35 at 50 mg/kg b.i.d.) (50 μl/25 g). All animals were weighed twice weekly to monitor the general health status (severity of infection and toxicity of medication). Amastigote burdens in the liver and spleen target organs were determined on days 16 and 17 of the experiment. Organs of individual animals were weighed, and impression smears were subjected to Giemsa staining for microscopic evaluation of the total amastigote burden (the mean number of amastigotes per cell × number of cells counted [minimum of 500 nuclei]). Percent reduction compared to the burdens in the vehicle-treated infected control animals was used as a measure of drug activity.

SUPPLEMENTAL MATERIAL

Supplemental material for this article may be found at https://doi.org/10.1128/AAC.00603-18.

SUPPLEMENTAL FILE 1, PDF file, 0.2 MB.

ACKNOWLEDGMENTS

We thank Pim-Bart Feijens, Margot Desmet, Mandy Vermont, and An Matheeussen for running the *in vitro* and *in vivo Leishmania* experiments.

Funding from the EC 7th Framework Programme (FP7-HEALTH-2013-INNOVATION-1, PDE4NPD no. 602666), MINECO (grant SAF2015-65740-R), RICET (RD16/0027/0010), FEDER funds, and MECD (grant FPU15/1465 to V.S.-P.) is acknowledged.

REFERENCES

1. Pace D. 2014. Leishmaniasis. J Infect 69(Suppl 1):S10–S18. https://doi.org/10.1016/j.jinf.2014.07.016.
2. Savoia D. 2015. Recent updates and perspectives on leishmaniasis. J Infect Dev Ctries 9:588–596. https://doi.org/10.3855/jidc.6833.
3. Alvar J, Vélez ID, Bern C, Herrero M, Desjeux P, Cano J, Jannin J, den Boer M; WHO Leishmaniasis Control Team. 2012. Leishmaniasis worldwide and global estimates of its incidence. PLoS One 7:e35671. https://doi.org/10.1371/journal.pone.0035671.
4. Alvar J, Aparicio P, Aseffa A, Den Boer M, Canavate C, Dedet JP, Gradoni L, Ter Horst R, Lopez-Velez R, Moreno J. 2008. The relationship between leishmaniasis and AIDS: the second 10 years. Clin Microbiol Rev 21:334–359. https://doi.org/10.1128/CMR.00061-07.
5. Srivastava S, Shankar P, Mishra J, Singh S. 2016. Possibilities and challenges for developing a successful vaccine for leishmaniasis. Parasit Vectors 9:277. https://doi.org/10.1186/s13071-016-1553-y.
6. Bates PA, Depaquit J, Galati EA, Kamhawi S, Maroli M, McDowell MA, Picado A, Ready PD, Salomon OD, Shaw JJ, Traub-Cseko YM, Warburg A. 2015. Recent advances in phlebotomine sand fly research related to leishmaniasis control. Parasit Vectors 8:131. https://doi.org/10.1186/s13071-015-0712-x.
7. Zulfiqar B, Shelper TB, Avery VM. 2017. Leishmaniasis drug discovery: recent progress and challenges in assay development. Drug Discovery Today 22:1516–1531. https://doi.org/10.1016/j.drudis.2017.06.004.
8. Nagle AS, Khare S, Kumar AB, Supek F, Buchynskyy A, Mathison CJ, Chennamaneni NK, Pendem N, Buckner FS, Gelb MH, Molteni V. 2014. Recent developments in drug discovery for leishmaniasis and human African trypanosomiasis. Chem Rev 114:11305–11347. https://doi.org/10.1021/cr500365f.
9. Skinner-Adams TS, Sumanadasa SD, Fisher GM, Davis RA, Doolan DL, Andrews KT. 2016. Defining the targets of antiparasitic compounds. Drug Discovery Today 21:725–739. https://doi.org/10.1016/j.drudis.2016.01.002.
10. de Koning HP. 2017. Drug resistance in protozoan parasites. Emerg Top Life Sci 1:627–632. https://doi.org/10.1042/ETLS20170113.
11. Maurice DH, Ke H, Ahmad F, Wang Y, Chung J, Manganiello VC. 2014. Advances in targeting cyclic nucleotide phosphodiesterases. Nat Rev Drug Discov 13:290–314. https://doi.org/10.1038/nrd4228.
12. Seebeck T, Sterk GJ, Ke H. 2011. Phosphodiesterase inhibitors as a new generation of antiprotozoan drugs: exploiting the benefit of enzymes that are highly conserved between host and parasite. Future Med Chem 3:1289–1306. https://doi.org/10.4155/fmc.11.77.
13. Shakur Y, de Koning HP, Ke H, Kambayashi J, Seebeck T. 2011. Therapeutic potential of phosphodiesterase inhibitors in parasitic diseases. Handb Exp Pharmacol 2011:487–510. https://doi.org/10.1007/978-3-642-17969-3_20.
14. Tagoe DN, Kalejaiye TD, de Koning HP. 2015. The ever unfolding story of cAMP signaling in trypanosomatids: vive la difference! Front Pharmacol 6:185. https://doi.org/10.3389/fphar.2015.00185.

15. Gould MK, Bachmaier S, Ali JA, Alsford S, Tagoe DN, Munday JC, Schnaufer AC, Horn D, Boshart M, de Koning HP. 2013. Cyclic AMP effectors in African trypanosomes revealed by genome-scale RNA interference library screening for resistance to the phosphodiesterase inhibitor CpdA. Antimicrob Agents Chemother 57:4882–4893. https://doi.org/10.1128/AAC.00508-13.
16. Salmon D, Vanwalleghem G, Morias Y, Denoeud J, Krumbholz C, Lhomme F, Bachmaier S, Kador M, Gossmann J, Dias FB, De Muylder G, Uzureau P, Magez S, Moser M, De Baetselier P, Van Den Abbeele J, Beschin A, Boshart M, Pays E. 2012. Adenylate cyclases of Trypanosoma brucei inhibit the innate immune response of the host. Science 337:463–466. https://doi.org/10.1126/science.1222753.
17. Makin L, Gluenz E. 2015. cAMP signalling in trypanosomatids: role in pathogenesis and as a drug target. Trends Parasitol 31:373–379. https://doi.org/10.1016/j.pt.2015.04.014.
18. de Koning HP, Gould MK, Sterk GJ, Tenor H, Kunz S, Luginbuehl E, Seebeck T. 2012. Pharmacological validation of Trypanosoma brucei phosphodiesterases as novel drug targets. J Infect Dis 206:229–237. https://doi.org/10.1093/infdis/jir857.
19. King-Keller S, Li M, Smith A, Zheng S, Kaur G, Yang X, Wang B, Docampo R. 2010. Chemical validation of phosphodiesterase C as a chemotherapeutic target in Trypanosoma cruzi, the etiological agent of Chagas' disease. Antimicrob Agents Chemother 54:3738–3745. https://doi.org/10.1128/AAC.00313-10.
20. Kunz S, Balmer V, Sterk GJ, Pollastri MP, Leurs R, Muller N, Hemphill A, Spycher C. 2017. The single cyclic nucleotide-specific phosphodiesterase of the intestinal parasite Giardia lamblia represents a potential drug target. PLoS Negl Trop Dis 11:e0005891. https://doi.org/10.1371/journal.pntd.0005891.
21. Gould MK, de Koning HP. 2011. Cyclic-nucleotide signalling in protozoa. FEMS Microbiol Rev 35:515–541. https://doi.org/10.1111/j.1574-6976.2010.00262.x.
22. Johner A, Kunz S, Linder M, Shakur Y, Seebeck T. 2006. Cyclic nucleotide specific phosphodiesterases of Leishmania major. BMC Microbiol 6:25. https://doi.org/10.1186/1471-2180-6-25.
23. Bhattacharya A, Biswas A, Das PK. 2008. Role of intracellular cAMP in differentiation-coupled induction of resistance against oxidative damage in Leishmania donovani. Free Radic Biol Med 44:779–794. https://doi.org/10.1016/j.freeradbiomed.2007.10.059.
24. Wang H, Yan Z, Geng J, Kunz S, Seebeck T, Ke H. 2007. Crystal structure of the Leishmania major phosphodiesterase LmjPDEB1 and insight into the design of the parasite-selective inhibitors. Mol Microbiol 66:1029–1038. https://doi.org/10.1111/j.1365-2958.2007.05976.x.
25. Castaño T, Wang H, Campillo NE, Ballester S, Gonzalez-Garcia C, Hernandez J, Perez C, Cuenca J, Perez-Castillo A, Martinez A, Huertas O, Gelpi JL, Luque FJ, Ke H, Gil C. 2009. Synthesis, structural analysis, and biological evaluation of thioxoquinazoline derivatives as phosphodiesterase 7 inhibitors. ChemMedChem 4:866–876. https://doi.org/10.1002/cmdc.200900043.
26. Redondo M, Brea JM, Perez DI, Soteras I, Val C, Perez C, Morales-Garcia JA, Alonso-Gil S, Paul-Fernandez N, Martin-Alvarez R, Cadavid I, Loza I, Perez-Castillo A, Mengod G, Campillo NE, Martinez A, Gil C. 2012. Effect of phosphodiesterase 7 (PDE7) inhibitors in experimental autoimmune encephalomyelitis mice. Discovery of a new chemically diverse family of compounds. J Med Chem 55:3274–3284. https://doi.org/10.1021/jm201720d.
27. Redondo M, Palomo V, Brea J, Perez DI, Martin-Alvarez R, Perez C, Paul-Fernandez N, Conde S, Cadavid MI, Loza MI, Mengod G, Martinez A, Gil C, Campillo NE. 2012. Identification in silico and experimental validation of novel phosphodiesterase 7 inhibitors with efficacy in experimental autoimmune encephalomyelitis mice. ACS Chem Neurosci 3:793–803. https://doi.org/10.1021/cn300105c.
28. García AM, Brea J, Morales-García JA, Perez DI, González A, Alonso-Gil S, Gracia-Rubio I, Ros-Simó C, Conde S, Cadavid MI, Loza MI, Perez-Castillo A, Valverde O, Martinez A, Gil C. 2014. Modulation of cAMP-specific PDE without emetogenic activity: new sulfide-like PDE7 inhibitors. J Med Chem 57:8590–8607. https://doi.org/10.1021/jm501090m.
29. García AM, Salado IG, Perez DI, Brea J, Morales-García JA, González-García A, Cadavid MI, Loza MI, Luque FJ, Perez-Castillo A, Martinez A, Gil C. 2017. Pharmacological tools based on imidazole scaffold proved the utility of PDE10A inhibitors for Parkinson's disease. Future Med Chem 9:731–748. https://doi.org/10.4155/fmc-2017-0005.
30. Sebastian-Pérez V, Roca C, Awale M, Reymond J-L, Martínez A, Gil C, Campillo NE. 2017. The Medicinal and Biological Chemistry (MBC) library: an efficient source on new hits. J Chem Infect Model 57:2143–2151. https://doi.org/10.1021/acs.jcim.7b00401.
31. Kaiser M, Maes L, Tadoori LP, Spangenberg T, Ioset JR. 2015. Repurposing of the Open Access Malaria Box for kinetoplastid diseases identifies novel active scaffolds against Trypanosomatids. J Biomol Screen 20:634–645. https://doi.org/10.1177/1087057115569155.
32. Veerman J, van den Bergh T, Orrling KM, Jansen C, Cos P, Maes L, Chatelain E, Ioset JR, Edink EE, Tenor H, Seebeck T, de Esch I, Leurs R, Sterk GJ. 2016. Synthesis and evaluation of analogs of the phenylpyridazinone NPD-001 as potent trypanosomal TbrPDEB1 phosphodiesterase inhibitors and in vitro trypanocidals. Bioorg Med Chem 24:1573–1581. https://doi.org/10.1016/j.bmc.2016.02.032.
33. Martinez A, Gil C. 2018. Medicinal chemistry strategies to discover new leishmanicidal drugs, p 153–178. *In* Rivas L, Gil C (ed), Drug discovery for leishmaniasis. Royal Society of Chemistry, Cambridge, United Kingdom.
34. Amata E, Xi H, Colmenarejo G, Gonzalez-Diaz R, Cordon-Obras C, Berlanga M, Manzano P, Erath J, Roncal NE, Lee PJ, Leed SE, Rodriguez A, Sciotti RJ, Navarro M, Pollastri MP. 2016. Identification of "Preferred" human kinase inhibitors for sleeping sickness lead discovery. Are some kinases better than others for inhibitor repurposing? ACS Infect Dis 2:180–186. https://doi.org/10.1021/acsinfecdis.5b00136.
35. Hughes JP, Rees S, Kalindjian SB, Philpott KL. 2011. Principles of early drug discovery. Br J Pharmacol 162:1239–1249. https://doi.org/10.1111/j.1476-5381.2010.01127.x.
36. Palomo V, Perez DI, Perez C, Morales-Garcia JA, Soteras I, Alonso-Gil S, Encinas A, Castro A, Campillo NE, Perez-Castillo A, Gil C, Martinez A. 2012. 5-Imino-1,2,4-thiadiazoles: first small molecules as substrate competitive inhibitors of glycogen synthase kinase 3. J Med Chem 55:1645–1661. https://doi.org/10.1021/jm201463v.
37. Cos P, Vlietinck AJ, Berghe DV, Maes L. 2006. Anti-infective potential of natural products: how to develop a stronger in vitro 'proof-of-concept'. J Ethnopharmacol 106:290–302. https://doi.org/10.1016/j.jep.2006.04.003.
38. Schrödinger, LLC. 2015. Schrödinger release 2015-4: LigPrep. Schrödinger, LLC, New York, NY.
39. Schrödinger, LLC. 2015. Schrödinger Suite 2015-4, including Protein Preparation Wizard, Epik, Impact, and Prime. Schrödinger, LLC, New York, NY.
40. Schrödinger, LLC. 2015. Schrödinger release 2015-4: Maestro. Schrödinger, LLC, New York, NY.
41. Morris GM, Goodsell DS, Halliday RS, Huey R, Hart WE, Belew RK, Olson AJ. 1998. Automated docking using a Lamarckian genetic algorithm and an empirical binding free energy function. J Comput Chem 19:1639–1662. https://doi.org/10.1002/(SICI)1096-987X(19981115)19:14<1639::AID-JCC10>3.0.CO;2-B.
42. Morris GM, Huey R, Lindstrom W, Sanner MF, Belew RK, Goodsell DS, Olson AJ. 2009. AutoDock4 and AutoDockTools4: automated docking with selective receptor flexibility. J Comput Chem 30:2785–2791. https://doi.org/10.1002/jcc.21256.
43. Banks JL, Beard HS, Cao Y, Cho AE, Damm W, Farid R, Felts AK, Halgren TA, Mainz DT, Maple JR, Murphy R, Philipp DM, Repasky MP, Zhang LY, Berne BJ, Friesner RA, Gallicchio E, Levy RM. 2005. Integrated Modeling Program, Applied Chemical Theory (IMPACT). J Comput Chem 26:1752–1780. https://doi.org/10.1002/jcc.20292.
44. Schrödinger, LLC. 2015. Schrödinger Release 2015-4: Desmond molecular dynamics system, Maestro-Desmond interoperability tools, D. E. Shaw Research. Schrödinger, New York, NY, 2015.
45. Schrödinger, LLC. 2015. Jaguar. Schrödinger release 2015-4: Jaguar. Schrödinger, LLC, New York, NY.
46. Humphrey W, Dalke A, Schulten K. 1996. VMD: visual molecular dynamics. J Mol Graph 14:33–38. https://doi.org/10.1016/0263-7855(96)00018-5.